Temperature-Induced Intermicellization of "Hairy" and "Crew-Cut" Micelles in an Aqueous Solution of a Thermoresponsive Copolymer

ARTICLE *in* LANGMUIR · JANUARY 2009

Impact Factor: 4.46 · DOI: 10.1021/la8030073 · Source: PubMed

4 AUTHORS, INCLUDING:

Kaizheng Zhu
University of Oslo
82 PUBLICATIONS **811** CITATIONS
SEE PROFILE

Ramón Pamies
Universidad Politécnica de Cartagena
24 PUBLICATIONS **333** CITATIONS
SEE PROFILE

Anna-Lena Kjøniksen
Østfold University College
122 PUBLICATIONS **2,336** CITATIONS
SEE PROFILE

Temperature-Induced Intermicellization of "Hairy" and "Crew-Cut" Micelles in an Aqueous Solution of a Thermoresponsive Copolymer

Kaizheng Zhu, Ramón Pamies, Anna-Lena Kjøniksen,* and Bo Nyström

Department of Chemistry, University of Oslo, P.O. Box 1033, Blindern, N-0315 Oslo, Norway

Received July 16, 2008. Revised Manuscript Received October 16, 2008

Temperature-induced intermicellar structures in aqueous solutions of the thermoresponsive methoxypoly(ethylene glycol)-*block*-poly(*N*-isopropylacrylamide) ($MPEG_n$-*b*-$NIPAAM_{71}$) copolymer that exhibit a lower critical solution temperature were studied by means of turbidimetry, dynamic light scattering (DLS), shear viscosity, and rheo small-angle light scattering (rheo-SALS) methods. The length of the hydrophilic chains (MPEG) of the copolymer varies from $n = 0$ to $n = 114$. It is shown that this change has a major impact on the temperature-induced association behavior of the polymer in solution. The turbidity results at quiescent conditions revealed a transition peak in the turbidity curve at intermediate temperatures, and this peak as well as the cloud point is shifted toward higher temperatures with increasing length of the hydrophilic chains of the copolymer. The DLS measurements disclosed a fast and a slow relaxation mode, which both are diffusive. From the fast and slow relaxation times the sizes of unimers/micelles and intermicellar clusters, respectively, can be determined. The temperature-induced aggregation is less pronounced in solutions of copolymers with long hydrophilic chains, and the intermicellar structures exhibit an interesting transition at intermediate temperatures. In the shear viscosity measurements large association complexes are formed at high temperatures and at low shear flow for the polymers with short hydrophilic chains, whereas at high shear rates breakup of interaggregate chains was observed. For the copolymer with the highest number of hydrophilic chains ($n = 114$), a novel transition peak was found in the viscosity data. The rheo-SALS results divulged shear-induced structural changes of the association complexes at elevated temperatures. For copolymers with short hydrophilic chains, shear-induced disruption of association complexes was found at higher temperatures, whereas for hairy micelles augmented shear flow promoted the growth of complexes.

Introduction

The self-assembly of asymmetric thermosensitive amphiphilic block copolymers has attracted a great deal of interest in recent years.[1−5] Self-assembled systems are suitable for a number of applications in nanotechnology, reusable elastomeric materials, electronics, and drug delivery.[5,6] Poly(*N*-isopropylacrylamide) (PNIPAAM) is a typical paradigm of a thermosensitive water-soluble polymer that exhibits a lower critical solution temperature (LCST),[7] below which the polymer is soluble and above which the molecules are in a collapsed state and the system approaches macroscopic phase separation.

In the present work, diblock copolymers containing the same number of NIPAAM units but with different lengths of the hydrophilic block monomethoxy-capped poly(ethylene glycol) (MPEG) were synthesized by utilizing atom transfer radical polymerization (ATRP). The prepared product is methoxypoly-(ethylene glycol)-*block*-poly(*N*-isopropylacrylamide) with the composition $MPEG_n$-*b*-$NIPAAM_{71}$, where n varies from 0 to 114. The chemical structure of the diblock copolymer is displayed in Figure 1.

Two extremes of micellar structures can be distinguished for amphiphilic diblock copolymers, depending on the relative length of the blocks. If the soluble block is much larger than the insoluble one, the formed micelles consist of a small core and a large corona; this type of architecture may be called "hairy" or "starlike" micelles.[8] On the other hand, if the micelles consist of a dominant hydrophobic core and a short hydrophilic corona, this structural design may be referred to as "crew-cut" micelles.[9] The basic idea behind the present study is that these different structures should respond to a temperature alteration in a different way because the hydrophobicity of the species is dissimilar, and the conjecture is that this leads to a higher sticking probability at elevated temperatures for the micelles with the shortest hydrophilic chains. Copolymers with long hydrophilic chains are foreseen to be less disposed to form intermicellar complexes at high temperatures because of the hydrophilic protective shell. This is still an open issue, and the preparation and characterization of these diblock copolymers in this work makes it possible to gain a novel insight into this problem both at quiescent conditions and under the influence of shear flow.

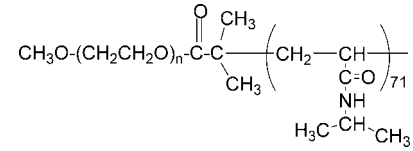

Figure 1. Chemical structure of the thermoresponsive $MPEG_n$-*b*-$NIPAAM_{71}$ diblock copolymer. The values of n for the investigated samples are 0, 12, 23, and 114.

In this work, we employed turbidity, light scattering, steady shear viscosity, and rheo small-angle light scattering (rheo-SALS) experiments to reveal spectacular differences in the behaviors between aqueous solutions of $MPEG_n$-*b*-$NIPAAM_{71}$ with different values of n. It is shown that, depending on the value of n, aqueous

(1) Muthukumar, M.; Ober, C. K.; Thomas, E. L. *Science* **1997**, *277*, 1225.
(2) Qiu, X.; Wu, C. *Macromolecules* **1997**, *30*, 7921.
(3) Förster, S.; Antonietti, M. *Adv. Mater.* **1998**, *10*, 195.
(4) *Responsive Polymer Materials: Design and Applications*; Minko, S., Ed.; Blackwell Publishing: Ames, IA, 2006.
(5) *Block Copolymers in Nanoscience*; Lazzari, M., Liu, G., Lecommandoux, S., Eds.; Wiley-VCH: Weinheim, Germany, 2006.
(6) Malmsten, M. *Surfactants and Polymers in Drug Delivery*; Marcel Dekker: New York, 2002.
(7) Schild, H. K. *Prog. Polym. Sci.* **1992**, *17*, 163.
(8) Price, C. In *Developments in Block Copolymers*, Goodman, I., Ed.; Applied Science Publishers: London, 1982; Vol. *1*, p 39.
(9) Halperin, A. *Macromolecules* **1990**, *23*, 2724.

10.1021/la8030073 CCC: $40.75
Published on Web 11/21/2008

solutions of the polymer can undergo a temperature-induced transition from loose intermicellar clusters to contracted core−shell nanostructures. The association properties of copolymers of this type have been studied previously.[10−14] There are, however, few studies on how the properties of these systems vary with the length of the different blocks. Motokawa et al.[12] have studied the effect of changing the length of the PNIPAAM group. Virtanen et al.[14] have varied the length of both blocks, but their PNIPAAM blocks are much longer than the ones used in this study (M_n(PNIPAAM) ≈ 340 000). As far as we know, this is the first study where the effect of varying the length of the MPEG group while keeping the size of the PNIPAAM group constant has been examined systematically.

In this paper we present some new results concerning temperature-induced crossover phenomena in aqueous solutions of this type of diblock copolymer, and it is demonstrated that the length of the hydrophilic block can modulate the temperature-induced changeover. The buildup and breakdown of intermicellar complexes under the influence of shear stresses are probed by rheo-SALS. The aim of this investigation is to elucidate the intricate interplay between hydrophilic and hydrophobic interactions during the influence of a temperature gradient.

Experimental Section

Materials, Synthesis, and Solution Preparation. All the chemicals used for the synthesis of the block copolymers were purchased from Aldrich and Fluka. The synthesis of the MPEG macroinitiators of various lengths was performed in accordance with a published procedure by the reaction of monomethoxyl-capped poly(ethylene glycol) ($MPEG_{12}$-OH, $MPEG_{23}$-OH, and $MPEG_{114}$-OH, and the data of M_n = 550, 1000, and 5000 were provided by the manufacturer) with 2-bromoisobutyryl bromide in the presence of triethylamine.[15] All polymers were synthesized by means of ATRP,[16,17] which was carried out in a water/DMF, 40:60 (v/v), mixture solvent at 25 °C via an ATRP system with MPEG macroinitiator (MI)/CuCl/Me_6TREN as the initiator/catalyst system except for the pure PNIPAAM where ethyl 2-chloropropionate (ECP) was used as the initiator to conduct the polymerization. The preparation and purification of these copolymers were conducted under similar conditions as described in our previous paper.[10] Typically, MPEG-MI (1 mmol) and NIPAAM (80 mmol) were dissolved in 40 mL of a water/DMF, 40:60 (v/v), solvent mixture ([NIPAAM] = 2.0 M) in a 100 mL Schlenk flask under magnetic stirring. The mixture was degassed by bubbling with argon for 30 min, before it was immersed in a water bath that was kept at about 25 °C. A volume of 2 mL of the freshly prepared Cu(I)−Me_6TREN water stock solution (prepared with degassed water (8 mL), CuCl (4 mmol), and Me_6TREN (4 mmol) under argon flow) was withdrawn via a syringe and quickly added to the above mixture, and the polymerization reaction was then initiated. When the NIPAAM monomer conversion reached approximately 95% (after approximately 1 h, ^{1}H NMR analysis indicated that more than 95% of the NIPAAM had been polymerized (disappearance of the vinyl signals at δ = 5.5−6.0 ppm), the product was then passed through an Al_2O_3 column (basic, activated) with THF as the eluent to remove Cu complexes. The polymer was further purified by dialyzing against distilled water for several days using a dialysis membrane of regenerated cellulose with a molecular weight cutoff of 3500. The white solid product was finally isolated by lyophilization.

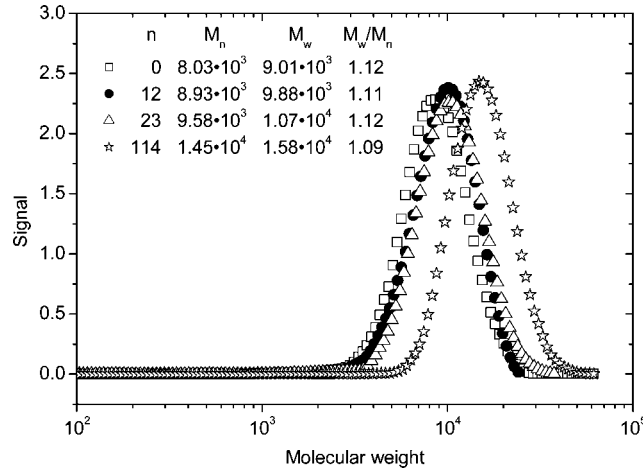

Figure 2. Illustration of the molecular weight distribution of the four $MPEG_n$-*b*-$NIPAAM_{71}$ block copolymers in aqueous solutions (0.01 M NaCl) with the aid of AFFFF. The values of n, M_n, M_w, and M_w/M_n of the copolymers are also indicated in the figure.

The chemical compositions and structures of the synthesized diblock copolymers were all ascertained by ^{1}H NMR with a Bruker Avance DPX 300 NMR spectrometer, operating at 300.13 MHz at 25 °C by utilizing heavy water as the solvent. The repeat units of two blocks (EG and NIPAAM) in the block copolymer MPEG-*b*-PNIPAAM were calculated from the integral values of the characteristic peak of NIPAAM (δ = 3.82 ppm, −C*H*(CH$_3$)$_2$, I_a), the typical peak of EG (δ = 3.70 ppm, −C*H*$_2$C*H*$_2$O−, I_b), and the typical peak of the methoxyl end group (δ = 3.30 ppm, C*H*$_3$O−, I_c) on the basis of the simple equation $n_{NIPAAM} = 3(I_a/I_c)$, $n_{EG} = 3I_b/4I_c$. Similarly, the number of NIPAAM units in the pure PNIPAAM was calculated from the integral values of the characteristic peak of NIPAAM (δ = 3.82 ppm, −C*H*(CH$_3$)$_2$, I_a) and the typical peak of the ethyloxyl (ECP) (δ = 4.20 ppm, CH$_3$C*H*$_2$O−, I_b) on the basis of another simple equation: $n_{NIPAAM} = 2(I_a/I_b)$. The weight-average molecular weights (M_w) and polydispersity indexes (M_w/M_n) of the copolymers were determined in dilute aqueous solutions by means of asymmetric flow field-flow fractionation (AFFFF) methods,[10,18] and the data from the measurements are collected in Figure 2. The experimental procedure and parameters are similar to what was reported previously.[10] It is noted that all polymer samples have low molecular weights and narrow molecular weight distributions. We note that the molecular weight of the sample increases in the expected way as the length of the hydrophilic chains increases.

All experiments were carried out at a fixed polymer concentration of 1 wt %, where micelles are formed and intermicellization occurs at elevated temperatures. The overlap concentration, c^*, can be estimated from[19] $c^* = 3M/4\pi N_A R_h^3$, where M is the molecular weight, N_A is Avogadro's constant, and R_h is the hydrodynamic radius. Using this equation at 25 °C, we find that c^* > 14 wt % for all the polymers used in this study. The polymer concentration of 1 wt % is therefore well into the dilute regime. We have also performed some measurements on a lower concentration (0.5 wt %) of the copolymers, but the features are practically the same; there are only some minor differences that do not alter the picture of the temperature-induced transitions. All samples were prepared by weighing the components, and the solutions were homogenized by being stirred for 1 day at ambient temperature.

Turbidimetry. Temperature dependences of the turbidity of the copolymer solutions were monitored at a heating rate of 0.2

(10) Zhu, K.; Jin, H.; Kjøniksen, A.-L.; Nyström, B. *J. Phys. Chem. B* **2007**, *111*, 10862.
(11) Zhang, W.; Shi, L.; Wu, K.; An, Y. *Macromolecules* **2005**, *38*, 5743.
(12) Motokawa, R.; Morishita, K.; Koizumi, S.; Nakahira, T.; Annaka, M. *Macromolecules* **2005**, *38*, 5748.
(13) Yan, J.; Ji, W.; Chen, E.; Li, Z.; Liang, D. *Macromolecules* **2008**, *41*, 4908.
(14) Virtanen, J.; Holappa, S.; Lemmetyinen, H.; Tenhu, H. *Macromolecules* **2002**, *35*, 4763.
(15) Liu, S.; Weaver, J. V. M.; Tang, Y.; Billingham, N. C.; Armes, S. P. *Macromolecules* **2002**, *35*, 6121.
(16) Hawker, C. J.; Bosman, A. W.; Harth, E. *Chem. Rev.* **2001**, *101*, 3661.
(17) Matyjaszewski, K.; Xia, J. *Chem. Rev.* **2001**, *101*, 2921.
(18) Modig, G.; Nilsson, L.; Bergenståhl, B.; Wahlund, K.-G. *Food Hydrocolloids* **2006**, *20*, 1087.
(19) Fleischer, G.; Puhlmann, A.; Rittig, F.; Konák, C. *Colloid Polym. Sci.* **1999**, *277*, 986.

°C/min by employing an NK60-CPA cloud point analyzer from Phase Technology, Richmond, BC, Canada. Detailed descriptions of the apparatus and determination of turbidities have been given elsewhere.[20] This instrumentation makes use of a scanning diffusive technique to characterize phase changes of the samples with high sensitivity and accuracy. The light beam from an AIGaAS light source, operating at 654 nm, was focused on the solution that was placed onto a specially designed glass plate that is coated with a thin metallic layer of very high reflectivity. Directly above the applied sample, an optical arrangement with a light scattering detector continuously monitors the scattered intensity signal (S) from the measured solutions as it is subjected to prescribed temperature alterations. A direct empiric relationship between the signal and the turbidity (τ) is found[20] to be $\tau = (9.0 \times 10^{-9})S^{3.751}$. All the data from the cloud point analyzer will be presented in terms of turbidity.

Dynamic Light Scattering. The dynamic light scattering (DLS) experiments were conducted with the aid of an ALV/CGS-8F multidetector compact goniometer system, with eight off fiber-optical detection units, from ALV-GmbH, Langen, Germany. The beam from a Uniphase cylindrical 22 mW He−Ne laser, operating at a wavelength of 632.8 nm with vertically polarized light, was focused on the sample cell (10 mm NMR tubes) through a temperature-controlled cylindrical quartz container (with two plane-parallel windows) and a vat (the temperature constancy being controlled to within ±0.01 °C with a heating/cooling circulator), which is filled with a refractive index matching liquid (*cis*-decalin). The polymer solutions were filtered through a 0.45 or 0.22 μm (the smallest filter is only used for the copolymer with the longest hydrophilic chains since the other polymers form large aggregates) filter (Millipore) directly into precleaned NMR tubes. The measurements were carried out under the influence of the same heating rate (0.2 °C/min) as for the turbidity and shear viscosity experiments. By this procedure the samples were exposed to the same history.

In the DLS measurements, the intensity correlation function was measured at eight scattering angles simultaneously in the range 22−141° with four ALV5000/E multiple-τ digital correlators. In the dilute concentration regime probed in this study, the scattered field obeys Gaussian statistics and the measured correlation function $g^2(q,t)$, where $q = (4\pi n/\lambda)\sin(\theta/2)$, with λ, θ, and n being the wavelength of the incident light in a vacuum, scattering angle, and refractive index of the medium, respectively, can be related to the theoretically amenable first-order electric field correlation function $g^1(q,t)$ by the Siegert relationship[21] $g^2(q,t) = 1 + B|g^1(q,t)|^2$, where B is usually treated as an empirical factor.

The correlation functions can be described by the sum of two stretched exponentials

$$g^1(t) = A_f \exp[-(t/\tau_{fe})^{\gamma}] + A_s \exp[-(t/\tau_{se})^{\beta}] \qquad (1)$$

with $A_f + A_s = 1$. The parameters A_f and A_s are the amplitudes for the fast and the slow relaxation times, respectively. The variables τ_{fe} and τ_{se} are the relaxation times characterizing the fast and the slow processes, respectively. This type of bimodal relaxation process has recently been reported[20,22,23] from DLS studies on aggregating polymer systems of various natures. In the analysis of the correlation functions by means of eq 1, a nonlinear fitting algorithm was employed to obtain best-fit values of the parameters A_f, τ_{fe}, τ_{se}, γ, and β appearing on the right-hand side of eq 1.

The fast mode is diffusive (q^2-dependent) for all samples, and it yields the mutual diffusion coefficient D ($\tau_f^{-1} = Dq^2$) of unimers. The slow mode (the second term on the right-hand side of eq 1) characterizes the dynamics of large clusters or intermicellar structures, and this mode is also found to be diffusive.

The parameters τ_{fe} and τ_{se} in eq 1 are effective relaxation times, and β ($0 < \beta \leq 1$) and γ ($0 < \gamma \leq 1$) are measures of the width of the distribution of relaxation times. The mean relaxation times for the fast and slow modes are given by

$$\tau_f = \frac{\tau_{fe}}{\gamma}\Gamma\left(\frac{1}{\gamma}\right) \qquad (2a)$$

$$\tau_s = \frac{\tau_{se}}{\beta}\Gamma\left(\frac{1}{\beta}\right) \qquad (2b)$$

where Γ is the Γ function. In this study we found that, depending on the stage of aggregation, the values of β and γ are in the intervals 0.8−1.0 and 0.9−1.0, respectively.

Shear Viscosity. A Paar-Physica MCR 300 rheometer, equipped with a cone-and-plate geometry with a cone angle of 1° and diameter of 75 mm, was utilized to monitor the shear viscosity of the polymer solutions. Even on dilute solutions, the rheometer operates effectively with this geometry, and the viscosity of water can readily be determined over an extended shear-rate domain. The solutions were introduced onto the plate, and to prevent evaporation of water, the free surface of the sample was always covered with a thin layer of low-viscosity silicone oil that virtually did not affect the solution viscosity. The instrument is equipped with a temperature unit (Peltier plate) that provides a fast and accurate alteration of the temperature over the studied temperature range. The temperature control is better than ±0.05 °C over the considered temperature domain. The measurements were conducted at a constant shear rate with a temperature gradient of 0.2 °C/min.

Rheo Small-Angle Light Scattering. Combined rheological and small-angle light scattering (rheo-SALS) experiments during shear flow were performed simultaneously using the Paar-Physica MCR 300 rheometer, equipped with a specially designed parallel plate−plate configuration (the diameter of the plate is 43 mm) in glass.[10] The instrumentation for the rheo-SALS experiments was purchased from Physica-Anton Paar. In all measurements a 10 mW diode laser operating at a wavelength of 658 nm was used as the light source, and a polarizer was placed in front of the laser and an analyzer below the sample, making both polarized (polarizer and analyzer parallel) and depolarized (polarizer and analyzer perpendicular) experiments possible. All experiments in this study were conducted using polarized light scattering. Utilizing a prism, the laser beam was deflected and passed through the sample placed between the transparent parallel plates. The distance between the plates is small (0.5 mm) so that the effect of multiple scattering is less pronounced when the sample becomes turbid at elevated temperatures. The light propagated along the velocity gradient direction, thus probing the structure in the plane of flow and vorticity. The forward scattered light at small angles was collected on a flat translucent screen below the sample (the distance between the sample and screen is 12.3 cm).

The 2D scattering patterns formed on the screen were captured using a CCD camera (driver LuCam V. 3.8), the plane of which is parallel to that of the screen. A Lumenera (VGA) CCD camera (Lumenera Corp., Ottawa, Canada) with a Pentax lens was utilized, and the scattered images were stored on a computer using the StreamPix (NorPix, Montreal, Quebec, Canada) application software (version 3.18.5), which enables a real-time digitalization of the images. The images were acquired via the CCD camera with an exposure time of 200 ms. Subsequently, the pictures were analyzed using the SALS software program (version 1.1) developed by the Laboratory of Applied Rheology and Polymer Processing, Department of Chemical Engineering, Katholieke Universiteit Leuven, Leuven, Belgium. The scattering functions were recorded continuously during the run. The approximate accessible scattering wave vector (q) range is between $q = 4 \times 10^{-4}$ nm^{-1} and $q = 2 \times 10^{-3}$ nm^{-1}.

Results and Discussion

In solutions of amphiphilic diblock copolymers the micellization process is essentially governed by the critical micelle

(20) Kjøniksen, A.-L.; Laukkanen, A.; Galant, C.; Knudsen, K. D.; Tenhu, H.; Nyström, B. *Macromolecules* **2005**, *38*, 948.
(21) Siegert, A. J. F. Radiation Laboratory Report No. 465; Massachusetts Institute of Technology: Cambridge, MA, 1943.
(22) Kjøniksen, A.-L.; Nyström, B.; Tenhu, H. *Colloids Surf., A* **2003**, *228*, 75.
(23) Chen, H.; Ye, X.; Zhang, G.; Zhang, Q. *Polymer* **2006**, *47*, 8367.

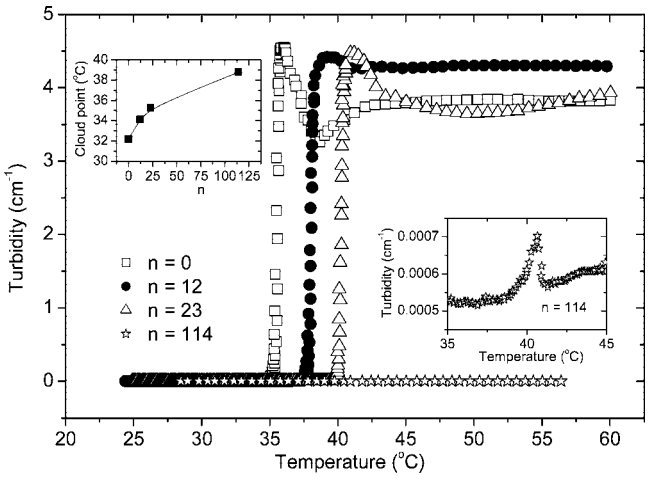

Figure 3. Temperature dependences of the turbidity during heating at a rate of 0.2 °C/min for 1 wt % solutions of MPEG$_n$-*b*-NIPAAM$_{71}$, with the indicated values of *n*. The upper inset shows the change of the cloud point with increasing value of *n*. The lower inset shows a magnification of the transition region for the sample with $n = 114$.

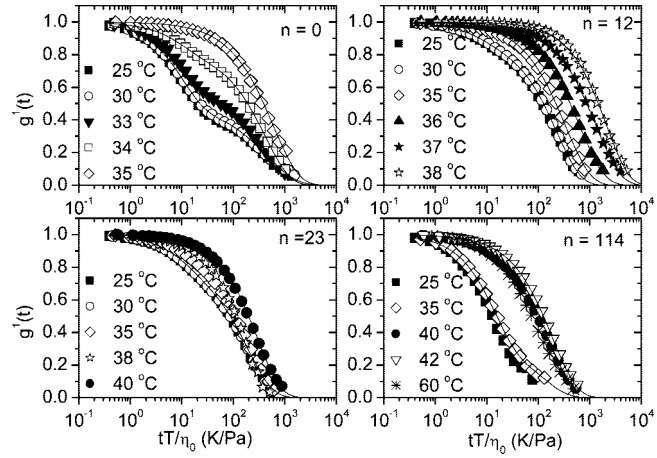

Figure 4. First-order field correlation function (at a scattering angle of 90°; every third data point is shown) versus the quantity tT/η for 1 wt % solutions of MPEG$_n$-*b*-NIPAAM$_{71}$ with the values of *n* indicated. The solid lines have been fitted with the aid of eq 1.

concentration (CMC) and the critical micelle temperature (CMT). Usually, the CMC for diblock copolymers is very low, and it can be difficult to determine it with conventional experimental methods.[5] If the polymer concentration is well below the conditions for the development of a CMC or CMT, self-assembly will not occur, the polymer will be molecularly dispersed in the solution, and the physical activities will be ruled by the unimers. At conditions where micelles are formed, they will be in thermodynamic equilibrium with the unimers. The constant polymer concentration (1 wt %) considered in this investigation is far above the CMC, which favors the development of micelles and intermicellar structures, especially at elevated temperatures. A temperature increase induces the clustering of individual micelles into larger association complexes, which may be characterized as loose micellar clusters.[24,25] In this work, the temperature-induced association features in solutions of the diblock copolymers, with the same number of hydrophobic groups but different thicknesses of the hydrophilic corona, are expected to vary depending on the length of the hydrophilic moieties. A thicker hydrophilic shell surrounding PNIPAAM should reduce the tendency of forming interchain aggregates at higher temperatures.

Turbidimetry. Turbidimetry is a powerful method to reveal the association behavior in solutions that exhibit a lower critical solution temperature. Figure 3 shows the effects of temperature on the turbidities at a heating rate of 0.2 °C/min for 1 wt % solutions of MPEG$_n$-*b*-NIPAAM$_{71}$ with values of *n* equal to 0, 12, 23, and 114. The temperature at which the first deviation of the scattered intensity from the baseline occurred was taken as the cloud point (CP), and it is evident from the upper inset that the value of CP increaseses with increasing length of the hydrophilic chains. The incipient rise of the turbidity with increasing temperature takes place at higher temperatures when the hydrophilic chains become longer because a higher temperature is needed to obtain the necessary stickiness for aggregation of the species. At intermediate temperatures a transition peak in the turbidity curve is observed for all systems, which reflects the temperature-induced formation of intermicellar-like structures and shrinking of the complexes at higher temperatures. This type of behavior has been reported previously for aqueous solutions of diblock and triblock copolymers.[26] We note that the peak is shifted toward higher temperatures as the number of hydrophilic groups in the polymer increases. The lower inset shows that even the solution of the copolymer with the longest hydrophilic chains exhibits a peak in the turbidity curve. However, the turbidity values are low in this case, and the intensity of aggregation is weak due to the longer hydrophilic chains.

Dynamic Light Scattering. Normalized time correlation function data at a scattering angle of 90° for 1 wt % solutions of MPEG$_n$-*b*-NIPAAM$_{71}$ with $n = 0$, 12, 23, and 114 under the influence of a temperature gradient are depicted in the form of semilogarithmic plots in Figure 4. To compare the results under the same conditions as employed for the turbidity and the viscosity experiments, the correlation functions were recorded continuously during heating at a rate of 0.2 °C/min. The solid lines have been fitted with the aid of eq 1, and the correlation functions are well described by this relation. To take into account trivial changes of the solvent viscosity with temperature, the correlation function data have been plotted against the quantity tT/η. Since both the fast and slow relaxation modes are diffusive, the effects of temperature on the relaxation processes will be analyzed in terms of apparent hydrodynamic radii.

The picture that emerges from these results is that the decay of the correlation function can initially be described by a single exponential, followed at longer times by a stretched exponential. Both relaxation modes are always diffusive (q^2-dependent), and this enables us to calculate the apparent hydrodynamic radii ($R_{h,f}$, and $R_{h,s}$)) from the fast and slow relaxation times, respectively, via the Stokes−Einstein relationship $R_h = k_BT/6\pi\eta D$, where k_B is the Boltzmann constant, T is the temperature, η is the solvent viscosity, and D is the diffusion coefficient of single micelles or intermicellar complexes.

In Figure 5, the temperature dependences of the apparent hydrodynamic radii derived from the fast relaxation time ($R_{h,f}$) and from the slow relaxation mode ($R_{h,s}$) are depicted for 1 wt % solutions of MPEG$_n$-*b*-PNIPAAM$_{71}$ with $n = 0$, 12, 23, and 114. In the temperature region of 25−40 °C, $R_{h,f}$ is in the range of 1.5−4 nm for all the considered polymers. This is close to

(24) Lysenko, E. A.; Bronich, T. K.; Slonkina, E. V.; Eisenberg, A.; Kabanov, V. A.; Kabanov, A. V. *Macromolecules* **2002**, *35*, 6351.
(25) Xu, R.; Winnik, M. A.; Hallett, F. R.; Riess, G.; Croucher, M. D. *Macromolecules* **1991**, *24*, 87.
(26) Kjøniksen, A.-L.; Zhu, K.; Pamies, R.; Nyström, B. *J. Phys. Chem. B* **2008**, *112*, 3294.

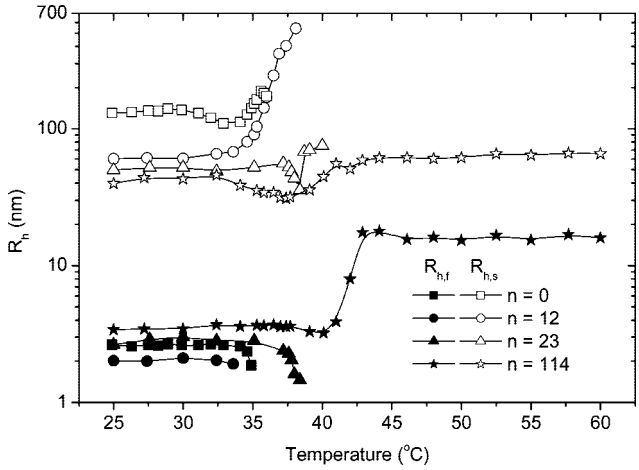

Figure 5. Temperature dependences of the apparent hydrodynamic radii determined from the fast relaxation time ($R_{h,f}$) and the slow relaxation time ($R_{h,s}$) through the Stokes−Einstein relation for 1 wt % solutions of MPEG$_n$-*b*-NIPAAM$_{71}$ with n = 0, 12, 23, and 114.

the sizes Movileanu et al.[27] reported for PEGs with molecular weights similar to those of the polymers used in this study, indicating that $R_{h,f}$ at these temperatures represents the size of the unimers. Motokawa et al.[12] determined the critical association concentration of PNIPAAM-*b*-PEG copolymers (M_n=9000−30000) to be 0.03−0.08 wt % and found that the hydrophobicity around pyrene probes started to increase around 17 °C. These findings are in agreement with the presence of a slow mode in 1 wt % MPEG$_n$-*b*-PNIPAAM$_{71}$ even at temperatures significantly below the cloud point. $R_{h,s}$ is much larger than $R_{h,f}$, suggesting that the slow mode is caused by intermicellar clusters. Except for the copolymer with the highest value of n, $R_{h,f}$ covers lower temperatures (higher temperatures are reached as the number of hydrophilic groups of the copolymer is increased) than the corresponding radii obtained from the slow relaxation mode, because when large clusters are formed in the solution, the impact of the unimers on the decay of the correlation function is small (a low value of the amplitude for the fast mode (A_f)) and it is not possible to extract the fast relaxation mode from the relaxation process. In this case, the decay of the correlation function is described by means of a single stretched exponential. A temperature-induced compression of the species is generally detected for the systems prior to the strong interchain association behavior sets in. This is a common effect that has been reported[20,28,29] for copolymers of various natures. A conspicuous feature is the sharp transition of $R_{h,f}$ at intermediate temperatures that is evident for the copolymer with the longest hydrophilic chains. We may note that the transition is located at approximately the same temperature as the maximum of the turbidity in the inset of Figure 3 for the same copolymer (n = 114). The initial decrease of $R_{h,f}$ is probably caused by contraction of the unimers, and the subsequent rise is due to the formation of micelles and probably some small clusters at higher temperatures, with structures where the long hydrophilic chains are protruding out from the hydrophobic inner part of the micelle into the bulk and thereby stabilizing the species from further interchain association at elevated temperatures.

Let us now discuss the temperature dependences of the apparent hydrodynamic radius obtained from the slow relaxation mode. At low temperatures, it is evident that the values of $R_{h,s}$ become gradually higher as the hydrophilic chains of the copolymer become shorter. This is ascribed to the higher sticking probability of species with shorter hydrophilic chains, and hence, the growth of the species is more marked. The apparent hydrodynamic radii ($R_{h,s}$) for the polymers with n = 0 and n = 12 exhibit a strong upturn at elevated temperatures; this trend reflects the enhanced growth of intermicellar structures. The solutions of these polymers approach macroscopic phase separation at high temperatures, and this effect in combination with enhanced multiple scattering prevents accurate DLS measurements in this temperature region. The solution of the diblock copolymer with n = 23 reveals a sharp minimum in $R_{h,s}$ at approximately 38 °C, and at temperatures above 40 °C the solution becomes very turbid (cf. Figure 3). This dip is attributed to contraction of the intermicellar structures before the omnipresent interchain aggregation process prevails at higher temperatures. In the case of the copolymer with n = 114, a broader minimum is observed than for the copolymer with n = 23. This is probably associated with the longer hydrophilic chains for this polymer. At temperatures beyond the minimum, only a modest increase in $R_{h,s}$ can be traced. This suggests that the long hydrophilic chains restrain the process of forming large intermicellar complexes at high temperatures.

When the samples become very turbid at high temperatures, we cannot analyze the correlation functions due to problems with multiple scattering. As the value of n increases and the cloud point is shifted toward higher temperatures (see Figure 3), we are able to determine $R_{h,s}$ at successively higher temperatures. $R_{h,s}$ decreases as the length of the hydrophilic MPEG group increases in the temperature range where we are able to analyze the correlation functions, but the size of the clusters we can measure before multiple scattering becomes a problem is different for each polymer, since this limit is dependent on several factors such as how rapidly the sample becomes turbid and the number and compactness of the clusters.

Shear Viscosity. In associating systems, a shear flow tends to bring polymer molecules and clusters close to each other faster than Brownian motion does, thereby speeding up the aggregation kinetics[30] of sticky species. This phenomenon of shear-induced intermolecular aggregation is known as "orthokinetic" aggregation, and it usually appears in solutions of sticky moieties at low shear rate, whereas at high shear rate, the large association complexes are foreseen to break up under the power of intensive shear stresses.[31−33] Under this condition, the growth rate of aggregates levels off or even decreases.

The effects of temperature and shear rate on the relative viscosity η_{rel} ($\eta_{rel} \equiv \eta/\eta_{water}$, with η_{water} being the solvent viscosity at a given temperature) for 1 wt % solutions of MPEG$_n$-*b*-NIPAAM$_{71}$ (n = 0, 12, 23, and 114) under the influence of a heating rate of 0.2 °C/min are illustrated in Figure 6. For the polymers with n = 0, 12, and 23, a pronounced upturn of the relative viscosity is a prominent feature at high temperatures and low shear rates; the amplitude of the upturn decreases as the length of the hydrophilic chains of the copolymer is increased. When the shear rate increases, the large clusters at high temperatures are broken up and only a modest temperature effect on η_{rel} is detected. A close inspection of the viscosity data for the polymers with n = 0 and 12 discloses a weak peak at intermediate temperatures. This peak probably reflects the

(27) Movileanu, L.; Cheley, S.; Bayley, H. *Biophys. J.* **2003**, *85*, 897.
(28) Lessard, D. G.; Ousalem, M.; Zhu, X X.; Eisenberg, A.; Carreau, P. J. *J. Polym. Sci., Part B: Polym. Phys.* **2003**, *41*, 1627.
(29) Chen, H.; Zhang, Q.; Li, J.; Ding, Y.; Zhang, G.; Wu, C. *Macromolecules* **2005**, *38*, 8045.
(30) Larson, R. G. *The Structure and Rheology of Complex Fluids*; Oxford University Press: New York, 1999.
(31) Doi, M.; Chen, D. *J. Chem. Phys.* **1989**, *90*, 5271; *91*, 2656.
(32) Brunet, E.; Degré, G.; Okkels, F.; Tabeling, P. *J. Colloid Interface Sci.* **2005**, *282*, 58.
(33) Potanin, A. A. *J. Colloid Interface Sci.* **1991**, *145*, 140.

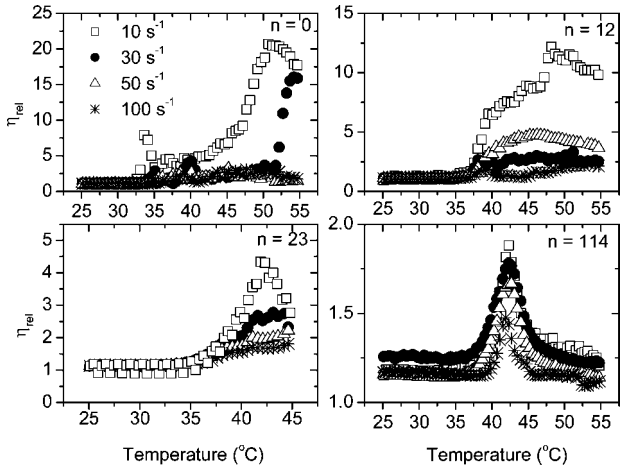

Figure 6. Effects of temperature and shear rate on the relative viscosity for 1 wt % solutions of MPEG$_n$-*b*-NIPAAM$_{71}$ with the indicated values of *n*.

formation of shear-induced association structures at temperatures where the sticking probability is lower. For the PNIPAAM solution ($n = 0$), a strong upturn of the relative viscosity is found at a shear rate of 30 s^{-1} at temperatures above 50 °C, and this seems to indicate that a moderate shear rate promotes the formation of large clusters of sticky molecules.

For the copolymer with $n = 114$, a marked transition peak appears at intermediate temperatures and its amplitude drops as the shear rate is increased. This peak can probably be associated with shear-induced intermicellization accompanied by contraction of the intermicellar structures at higher temperatures. The decrease of the amplitude of the peak with increasing shear rate indicates shear-induced aggregate breakup.

Rheo-SALS. This type of technique can provide us with information about structural changes of complexes on a global dimensional scale under the influence of shear flow. Figure 7 illustrates the 2D patterns of the scattered intensity at 30 and 40 °C at different shear rates for 1 wt % solutions of MPEG$_n$-*b*-NIPAAM$_{71}$ ($n = 0$, 12, 23, and 114). At higher temperatures, we encountered a similar problem with strong multiple scattering as discussed above in the context of the DLS experiments. The SALS images show that the overall scattered intensity increases with increasing temperature and the scattered patterns in the vorticity plane are virtually isotropic at all the studied shear rates for all systems; the black circle at the center of each pattern is the beam stop. The general picture that emerges is that for solutions of the diblock copolymer with relatively long hydrophilic chains ($n = 23$ and 114) shear-induced structures are formed at both 30 and 40 °C. The structure for the homopolymer ($n = 0$) that is visible in the quiescent state at 30 °C disappears at higher shear rates, whereas at 40 °C the scattered intensity is practically independent of the shear rate. For the copolymer with $n = 12$, it is obvious at 40 °C that the association complexes formed at quiescent conditions or at low shear rates are broken up at high shear flows.

The effects of temperature and shear rate on the scattered intensity (at a fixed *q* value of 0.20 μm^{-1}) for 1.0 wt % MPEG$_n$-*b*-NIPAAM$_{71}$ ($n = 0$, 12, 23, and 114) solutions are depicted in Figure 8. The general trend for the polymers with $n = 0$, 12, and 23 is that the intensity exhibits a steep rise over a narrow temperature interval and the curves gradually level out at elevated temperatures. For the homopolymer ($n = 0$), there is a small shear-induced breakup of the aggregates in the pretransition region and at higher temperatures no effect of shear flow can be discerned.

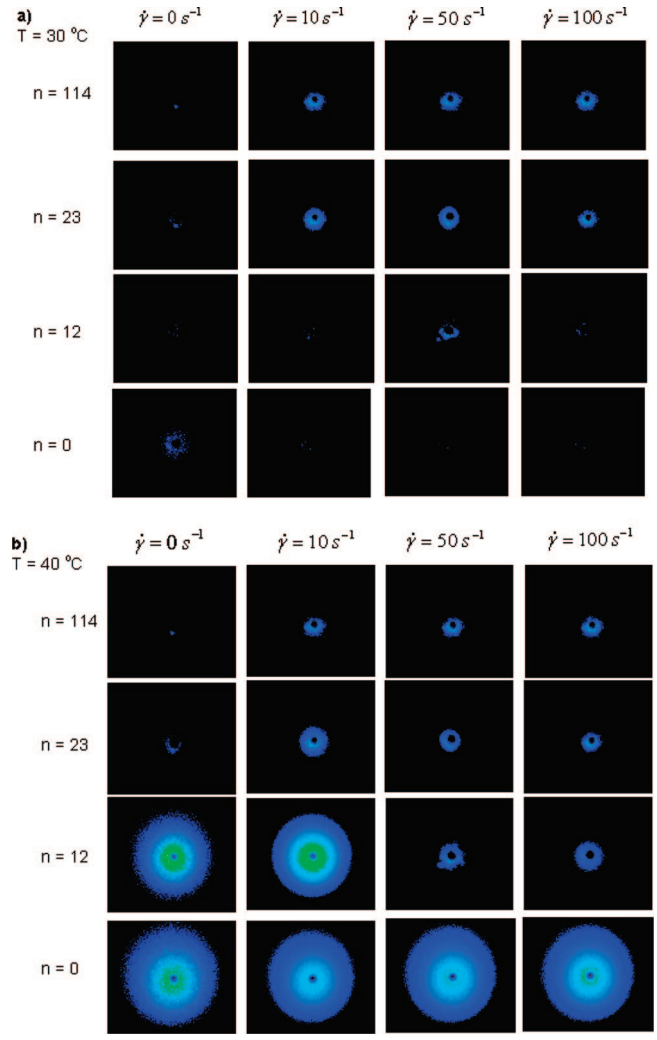

Figure 7. Scattered intensity patterns at the shear rates, temperatures, and values of *n* indicated for 1 wt % MPEG$_n$-*b*-NIPAAM$_{71}$ solutions.

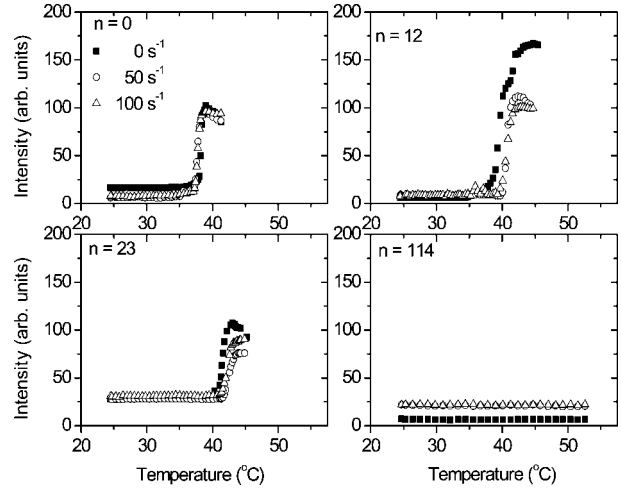

Figure 8. Effects of temperature and shear rate on the scattered intensity (at a fixed *q* value of 0.20 μm^{-1}) for 1 wt % MPEG$_n$-*b*-NIPAAM$_{71}$ solutions at the shear rates and values of *n* indicated.

For the copolymers with $n = 12$ and $n = 23$, shear stresses generate destruction of flocs at higher temperatures. For the copolymer with the longest hydrophilic chains a different scenario appears. In this case, no growth of aggregates at a constant shear

rate is detected over the considered temperature region and the scattered intensity increases with increasing shear flow. This suggests that the higher collision frequency between the species generates enhanced sticking probability, and this process leads to the formation of aggregates. This is a harbinger that the long hydrophilic chains protect the hydrophobic core from the adjacent entities, but at higher shear flow the species are deformed and interchain association occurs.

Conclusions

The influence of shear flow and temperature on the association behavior in aqueous solutions of the amphiphilic copolymer with different lengths ($n = 0-114$) of the hydrophilic chains was studied with the aid of turbidity, dynamic light scattering, shear viscosity, and rheo-SALS. The cloud point and the turbidity transition are shifted toward higher temperature as the thickness of the hydrophilic corona increases. The fast and the slow modes are both diffusive; the fast mode provides information about the size of the unimers (and at high temperatures for $n = 114$, micelles), and the size of intermicellar complexes can be estimated from the slow relaxation time. Strong interchain associations are found for polymers with short hydrophilic chains at elevated temperatures, whereas for more hydrophilic copolymers an anomalous minimum is detected at intermediate temperatures.

The steady shear viscosity measurements under the influence of a low shear rate disclose the formation of large association structures in solutions of polymers with short hydrophilic chains at higher temperatures, and these interaggregate chains break up at high shear flow. For solutions of copolymers with longer hydrophilic chains the temperature-induced aggregation is less marked and a distinct transition peak at intermediate temperatures is observed for the copolymer with the longest hydrophilic chains. The amplitude of this peak decreases with increasing shear rate, which indicates that the origin of this peak can be attributed to the formation of intermicellar complexes.

The results from rheo-SALS show that for the homopolymer ($n = 0$) at higher temperatures (40−50 °C) the scattered intensity is practically unaffected by the applied shear rate, whereas for the copolymer with $n = 12$ fragmentation of the complexes occurs at higher shear rates at 40 °C. For the copolymer with the longest hydrophilic chains and the copolymer with $n = 23$, shear flow promotes the formation of association structures at 40 °C. For the copolymer with the longest hydrophilic chains, shear-induced growth of the complexes is found, and this behavior is attributed to the higher collision frequency of the species under the influence of shear flows.

The overall picture that emerges from this study is the following. At low temperature, the solutions, depending on the length of the hydrophilic chains, contain unimers, micelles, and intermicellar complexes. The complexes are significantly larger for the polymer without MPEG ($n = 0$), since these species cannot be stabilized by the hydrophilic MPEG groups. When the temperature is increased, NIPAAM becomes gradually more hydrophobic. This causes both the clusters and the single molecules to contract. A further increase in temperature causes an enhanced aggregation in the samples (provided that the hydrophilic chains in the copolymer are not too long), the number of free unimers is decreased, and the intermicellar structures grow. At this stage, the samples become turbid, except the polymer species with the longest MPEG chains that are stabilized by the hydrophilic groups. In this sample we observe the formation of micelles at high temperatures. When the temperature of the turbid samples is further increased, there is a competition between aggregation and contraction of the clusters, and a decrease in the turbidity is observed, indicating that there is probably an overall shrinking of the aggregate size. When shear is applied to the aggregates, they break down into smaller clusters.

The findings from this work clearly demonstrate that the intensity of intermolecular association can be significantly weakened when long hydrophilic chains surround the hydrophobic core. In this spirit, amphiphilic copolymers can be prepared with tunable associative properties. The results show that, for this type of copolymer, interplay between intermicellization and contraction of structures plays a prominent role. The rheological measurements illustrate that shear flow can both stimulate the formation of complexes and restrain the development of intermicellar structures.

Acknowledgment. We gratefully acknowledge support from the Norwegian Research Council for Projects 177665/V30 and 177556/V30. R.P. acknowledges a postdoctoral fellowship from Fundación Séneca-CARM.

LA8030073